Strongly coupled rotational band in ^{33}Mg

A. L. Richard *et al.*

Phys. Rev. C **96**, 011303 — Published 28 July 2017

DOI: 10.1103/PhysRevC.96.011303

Strongly Coupled Rotational Band in ^{33}Mg

A. L. Richard[1],* H. L Crawford[1,2],† P. Fallon[2], A. O. Macchiavelli[2], V. M. Bader[3,4], D. Bazin[3], M. Bowry[3], C. M. Campbell[2], M. P. Carpenter[5], R. M. Clark[2], M. Cromaz[2], A. Gade[3,4], E. Ideguchi[6], H. Iwasaki[3,4], M. D. Jones[2], C. Langer[3], I. Y. Lee[2], C. Loelius[3,4], E. Lunderberg[3,4], C. Morse[3,4], J. Rissanen[2], M. Salathe[2], D. Smalley[3], S. R. Stroberg[3,4], D. Weisshaar[3], K. Whitmore[3,4], A. Wiens[2], S. J. Williams[3], K. Wimmer[7], and T. Yamamato[6]

[1]*Institute for Nuclear and Particle Physics, Department of Physics and Astronomy, Ohio University, Athens, OH USA*
[2]*Nuclear Science Division, Lawrence Berkeley National Laboratory, Berkeley, CA 94720, USA*
[3]*National Superconducting Cyclotron Laboratory, Michigan State University, East Lansing, MI 48824, USA*
[4]*Department of Physics and Astronomy, Michigan State University, East Lansing, MI 48824, USA*
[5]*Physics Division, Argonne National Laboratory, Argonne, IL 60439, USA*
[6]*RCNP, Osaka University, Mihogakoa, Ibaraki, Osaka 567-0047, Japan and*
[7]*Department of Physics, The University of Tokyo, Bunkyo-ku, Tokyo 113-0033, Japan*

The "Island of Inversion" at $N \sim 20$ for the neon, sodium, and magnesium isotopes has long been an area of interest both experimentally and theoretically due to the subtle competition between $0p$-$0h$ and np-nh configurations leading to deformed shapes. However, the presence of rotational band structures, which are fingerprints of deformed shapes, have only recently been observed in this region. In this work, we report on a measurement of the low-lying level structure of ^{33}Mg populated by a two-stage projectile fragmentation reaction and studied with GRETINA. The experimental level energies, ground state magnetic moment, intrinsic quadrupole moment, and γ-ray intensities show good agreement with the strong-coupling limit of a rotational model.

PACS numbers:

I. INTRODUCTION

While it is well-known that the spherical Shell Model reproduces the experimental evidence for "magic" numbers near stability, neutron-rich nuclei with extreme proton (Z) to neutron (N) ratios have shown deviations from this description. The "Island of Inversion" centered at $N = 20$ for the neon, sodium, and magnesium isotopes is one such region, where rather than spherical nuclei expected from the $N = 20$ harmonic oscillator closure, one finds nuclei dominated by deformed ground states [1]. The reduction in the $N = 20$ shell gap in the region centered around ^{32}Mg favors the promotion of pairs of neutrons from the sd-shell into the pf-shell, as the promoted particles and sd-shell holes experience the quadrupole-quadrupole force and the gain in correlation energy overcomes the cost of crossing the gap. As such, nuclei are characterized by n-particle-n-hole (np-nh) excitations and deformation in their ground states. Many studies have been performed in this region [2–9], both experimentally and theoretically, which support and provide evidence for collective deformed ground states. Recently, a rotational structure, the fingerprint of deformed shapes, has been observed in ^{32}Mg up to spin $I = 6^+$, confirming this interpretation [10].

With one neutron coupled to ^{32}Mg, it would be reasonable to expect that ^{33}Mg will also be well deformed. This odd-A system can provide further insight into the rotational picture, the blocking of pairing correlations, and the stability of deformation. It will also be of interest to understand how rotational properties are modified by the effect of Coriolis coupling. In fact, the ground state magnetic moment of ^{33}Mg supports this picture, being in good agreement with the value expected for a valence neutron coupled to a prolate axially symmetric rotor [11–13], but a more extensive description of ^{33}Mg in this framework has yet to emerge.

In this Rapid Communication, we report on the results of a measurement of ^{33}Mg, identifying a low-lying rotational band structure in this isotope, and discuss the interpretation of this structure in the limit of the rotational model. ^{33}Mg was produced in a two-stage projectile fragmentation reaction and excited states were observed using the γ-ray tracking array GRETINA (Gamma Ray Energy Tracking In-beam Nuclear Array) [14]. The technique adopted, involving removal of a large number of nucleons from the secondary beam, provides a mechanism to populate higher angular momentum (I), especially in comparison to few nucleon removal reactions. In this work, the removal of 13 nucleons from a radioactive beam of ^{46}Ar was used to produce ^{33}Mg.

II. EXPERIMENTAL DETAILS

In the same experiment as described in Ref. [10], ^{33}Mg was produced and studied. A secondary beam of ^{46}Ar was produced at the National Superconducting Cyclotron Laboratory (NSCL) at Michigan State University from a primary beam of ^{48}Ca accelerated to 140 MeV/u and fragmented on a 846 mg/cm^2 thick ^{9}Be target located at

*Electronic address: ar286106@ohio.edu
†Electronic address: hlcrawford@lbl.gov

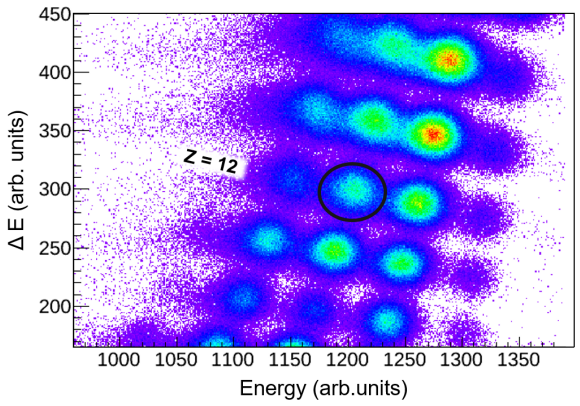

Figure 1: The fragments were identified using energy loss and total kinetic energy measurements from the S800 focal plane detector suite. The magnesium isotopes at $Z = 12$ are highlighted, with ^{33}Mg highlighted with a black circle.

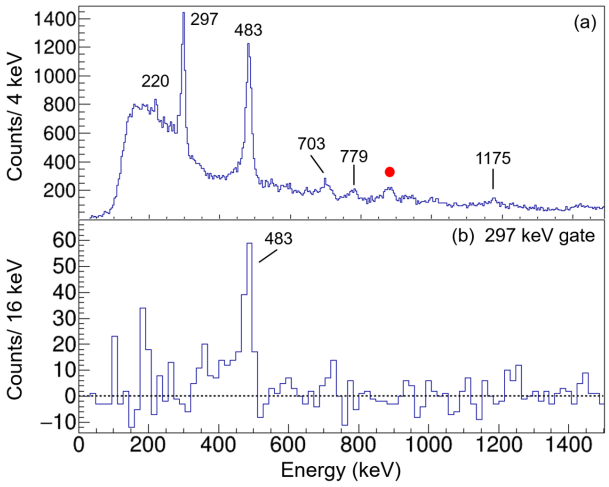

Figure 2: The Doppler reconstructed γ-ray spectrum of ^{33}Mg (a) detected with GRETINA (using clustering) following the secondary fragmentation of the beam. Transitions in ^{33}Mg are marked with their energies in black; the transition marked with a red circle corresponds to a γ-ray in the neighboring isotope, ^{32}Mg. The transition at 1175 keV corresponds to a weak, unplaced transition in ^{33}Mg. Panel (b) shows the background-subtracted, clustered $\gamma - \gamma$ projection of the 297 keV γ-ray. Clear coincidence can be seen with the 483 keV ground state transition.

the entrance of the A1900 fragment separator [15]. The ^{46}Ar secondary beam was separated from other fragments through the A1900 based on magnetic rigidity and energy loss through an Al wedge degrader located at the intermediate image.

The ^{46}Ar beam was transported to the S3 experimental vault with a momentum acceptance ($\Delta p/p$) of 1% and an energy of 102 MeV/u. A cocktail of secondary fragmentation products, including ^{33}Mg, were produced by fragmentation of the ^{46}Ar on a 267 mg/cm^2 thick ^{9}Be target located at the target position of the S800 spectrograph [16]. Fragments were identified on an event-by-event basis through their energy loss (ΔE) and total kinetic energy (E) as measured in the S800 focal plane detector suite [17, 18]. The E measurement was obtained using the CsI hodoscope [18]. To obtain a consistent particle ID across the array, individual hodoscope crystals were gain-matched to align the peaks corresponding to the $Z = 12$ Mg isotopes. The $E - \Delta E$ particle identification (PID) is shown in Figure 1 illustrating clear separation between isotopes at the S800 focal plane.

Prompt γ-rays were detected by seven GRETINA modules that surrounded the S800 target position. Each module was placed at 90° with respect to the beam direction in order to minimize beam-induced backgrounds from light particles produced in the high-intensity secondary fragmentation, which are forward focused in the laboratory frame. The high segmentation and digital pulse-shape processing of GRETINA allows the interaction energies and positions to be measured with sub-segment resolution. Utilizing the γ-ray trajectories from GRETINA and particle trajectories from the S800, γ-rays emitted from the fragmentation products (with $v/c = 0.4$) were Doppler reconstructed on an event-by-event basis, achieving an energy resolution (FWHM) of ∼2%. A GEANT4 simulation of the GRETINA response using the UCGretina code [19], combined with a smooth double-exponential function, was used to fit the background to allow accurate determination of γ-ray yields without constraining the peak shape. These yields were efficiency corrected based upon the simulated array efficiencies including the Lorentz boost.

III. RESULTS

The γ-ray singles spectrum observed in GRETINA in coincidence with identified ^{33}Mg nuclei is shown in the upper panel of Figure 2. Two strong transitions are observed at 297(4) and 483(4) keV with three weaker transitions at 220(4), 703(4), and 779(4) keV. The 220, 483, and 703 keV transitions correspond to γ-rays known and placed from previous work [7, 20–24]. The 483 keV γ-ray was placed as a transition directly to the tentative $3/2^-$ ground state [11], as was the 703 keV γ-ray [7, 21]. The 220 keV has been established to be in coincidence with the 483 keV transition [21], depopulating the 703 keV state.

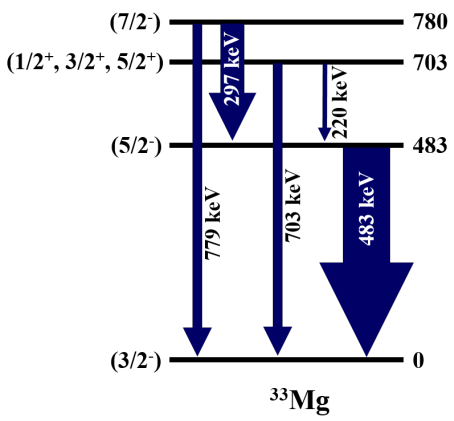

Figure 3: The level scheme of ^{33}Mg based upon γ-ray singles, $\gamma-\gamma$ coincidence data, and literature placements. The width of the arrows is representative of the relative intensity of the transition. All γ-ray transitions were measured with 4 keV uncertainty.

The 297 keV γ-ray was previously reported [21], but was not placed in the level scheme. In this work, the 297 keV was observed strongly and shown to be in coincidence with the 483 keV line through a $\gamma-\gamma$ analysis, as shown in the lower panel of Figure 2. Based on this coincidence relationship, and the observation of a weak transition at 779 keV, a new level is placed at 780(6) keV. A weak transition was observed at 1175(4) keV, but with the low statistics and lack of coincidence information, we cannot place it in the level scheme for ^{33}Mg. No additional transitions were observed above 1.5 MeV. The level scheme established in this work is shown in Figure 3. The ^{33}Mg experimental level energies, γ-ray energies, and tentative spin assignments (based upon the literature and arguments in the following section) are summarized in Table I.

Table I: Experimental level information for the low-lying states in ^{33}Mg as populated in the present work. Spin/parity assignments are tentative.

Initial State (keV)	I^π	Final State (keV)	I^π	E_γ (keV)	I_γ (rel. %)
780(6)	$^7/_2^-$	0	$^3/_2^-$	779(4)	12(4)
780(6)	$^7/_2^-$	483(4)	$^5/_2^-$	297(4)	48(13)
703(4)		0	$^3/_2^-$	703(4)	13(4)
703(4)		483(4)	$^5/_2^-$	220(4)	8(2)
483(4)	$^5/_2^-$	0	$^3/_2^-$	483(4)	100
				1175(4)	18(6)

IV. DISCUSSION

A natural starting point for the description of ^{33}Mg is to describe this nucleus as a ^{32}Mg core plus a valence neutron (or a ^{34}Mg core plus a valence hole). The low-lying yrast structure in ^{32,34}Mg is described as a rotational band [10] – the extension of this property from the even system to the odd system in ^{33}Mg is of interest for our understanding of the stability of deformation in this region. To this end, the low-energy excitation energies, γ-ray intensities, and other available data for ^{33}Mg are compared to a leading order rotational interpretation.

In deformed odd-A systems, low-lying states can be classified as rotational band states with each band having $I = K, K+1, K+2, ...$, where I is the spin of a particular level and K is the angular momentum of the bandhead (or the projection of the total angular momentum onto the nuclear symmetry axis). The coupling of the valence nucleon (a neutron, in this case) can be described by the relationship between the rotational energy of the odd-neutron compared to the excitation energy of the core. We consider here the experimental signatures of ^{33}Mg in the strong-coupling limit, where the rotational frequency is small compared to that of the single-particle and the motion of the odd-neutron follows the motion of the core.

In the following analysis we assume a $K = 3/2$ bandhead, arising from the unpaired neutron in the Nilsson 3/2[321] orbitals, which is consistent with the $3/2^-$ ground state adopted in the literature and the ground state magnetic moment [11, 25]. Assuming a strongly coupled structure built on this bandhead, we tentatively assign the levels at 483 keV and 780 keV as $5/2^-$ and $7/2^-$, respectively. These assumptions are supported by the strong population of these levels in this reaction, which is expected to favorably populate the yrast levels as was observed in ^{32}Mg [10], and by the energy of the first excited state, which is significantly less than the 2^+ state in the ^{32,34}Mg core.

A. Excitation Energies

The experimental excitation energies provide a first test of the leading order description for ^{33}Mg in the strong coupling limit. To a good approximation, the excitation energies for members of an even-even rotational band ($K = 0$) can be written as

$$E(I) = [AI(I+1) + BI^2(I+1)^2 + ...], \qquad (1)$$

where A and B are constants related to the moment-of-inertia [26]. Within a particular band, A is equivalent to $\hbar^2/2\mathscr{I}$, where $\mathscr{I}$ is the moment-of-inertia, and B represents a first-order correction describing the dependence of the moment-of-inertia on I. Past experimental data on the collective nature of ^{32}Mg found four levels in the ground state rotational band, namely a 0^+ state, a 2^+ state at 886(4) [10, 27–31], a 4^+ at 2324(6) [10, 32], and a 6^+ at 4097(7) [10]. Based upon these energies and spin assignments, the experimental energy sequences were fit to Eq. 1, and the values for A and

B were found to be 141.5(5) keV and -1.06(1) keV, respectively. Following the same analysis for the known levels in ^{34}Mg [20, 23, 31, 33], we obtain $A = 111.6(17)$ keV and B = -0.27(11) keV, indicating a slightly more rigid deformation in ^{34}Mg, but an overall consistent picture of these nuclei.

Moving to the odd particle case and treating ^{33}Mg in the strong coupling limit, an additional term must be added to the rotational energy shown in Eq. 1 arising from the Coriolis interaction that induces $\Delta K = \pm 2K$ coupling to account for the odd neutron as

$$\Delta E_{rot} = (-1)^{I+K} A_{2K} \frac{(I+K)!}{(I-K)!}, \quad (2)$$

where A_{2K} represents the Coriolis interaction strength and describes how the valence particle couples to the core [26]. From Table I, assuming that the strongly populated levels at 483 keV and 780 keV are members of the band, we obtain values of $A = 109.9(1)$ keV, B = -1.90(4) keV, and $A_3 = 1.74(6)$ keV.

The value of A for ^{33}Mg is reduced by 22% from that in ^{32}Mg. This is in good agreement with the expectations of pair-blocking by the odd-neutron reducing the pairing correlations in the core and resulting in a larger moment-of-inertia. The value of A_{2K} can be calculated directly from the intrinsic rotational Hamiltonian, $A_3 = \langle 3/2|h_3|\overline{3/2}\rangle$ [26]. For our particular case we have:

$$A_3 = -A^3 \frac{\langle 3/2|j_+|1/2\rangle\langle 1/2|j_+|\overline{1/2}\rangle\langle\overline{1/2}|j_+|\overline{3/2}\rangle}{(E_{1/2} - E_{3/2})^2}. \quad (3)$$

Using the relevant j_+ matrix elements, calculated with the standard Nilsson model [34, 35] at a deformation of 0.45 (see next section), we obtain $A_3 \approx 1.75$ keV, which reproduces the A_3 value from the experimental energy levels. The agreement with the experimental energy sequences suggests that to leading order, the rotational model provides a reasonable description of the states in ^{33}Mg (with the tentative spin and parity assignments) in Table I.

B. B($E2$), Magnetic Moment, and Intensity Ratio

Beyond excitation energies, the strong-coupling limit of the rotational model can be used to make specific predictions regarding observables including transition rates and nuclear moments. To further test the applicability of this description for ^{33}Mg, we consider additional experimental observables, namely the intensity ratio of the γ-rays depopulating the candidate $(7/2^-)$ state, the ground-state magnetic moment, μ [11], and the Q_0 derived from a measured $B(E2)$ [22].

The ratio of the γ-ray intensities between the $E2$ and $M1$ transitions depopulating the candidate $(7/2^-)$ state, denoted as λ is determined in the present work. This model assumes pure $E2$ and $M1$ transitions. Based upon the intensities of the transitions de-exciting from the 780 keV level, as shown in Table I, the experimental $E2$ to $M1$ ratio, λ_{exp}, is determined to be 0.24±0.08. The magnetic moment is known from the literature to be -0.7456(5)μ_N based upon laser spectroscopy and nuclear magnetic resonance measurements [11].

A Coulomb excitation measurement of ^{33}Mg on a gold target [22] determined a $B(E2\uparrow)$ of 232(107) e^{2}fm^4. However, this work assumed a $5/2^+$ ground state and excitation both directly to a $7/2^+$ state and an unobserved $9/2^+$ state. Their quoted uncertainties on the excitation strengths also took into account the possibility that the $9/2^+$ state may decay to the $7/2^+$ state anywhere from 0% to 100% of the time. Now assuming a $3/2^-$ ground state, Coulomb excitation should populate the $7/2^-$ state. With our proposed level scheme and branching ratios, one expects a Coulomb excitation spectrum with dominant 483 keV and 297 keV transitions corresponding to the depopulating two gamma cascade. This is consistent with the spectrum of Ref. [22], for which the low-energy background is likely obscuring the 297 keV transition. Based on the measured B($E2$) value, and the excitation scenario described above, we can extract a Q_0 value of 0.7(0.16) eb.

For a $K \neq 1/2$ band, λ can be expressed in terms of the γ-ray energies (in MeV), the g-factors (g_K and g_R), and the intrinsic quadrupole moment, Q_0:

$$\lambda = \Big[\frac{E_\gamma}{E_{\gamma'}}\Big]^5 \frac{(I+1)(I-1+K)(I-1-K)/2K^2(2I+1)}{1+1.148[(g_K-g_R)/Q_0]^2(I+1)(I-1){E_{\gamma'}}^{-2}}, \quad (4)$$

where $E_{\gamma'}$ refers to the energy of the $M1(+E2)$ transition, and E_γ to the energy of the $E2$ transition depopulating the same initial state [26]. The magnetic moment, μ, depends on the values for g_K and g_R and can be written as [26]

$$\frac{\mu}{I} = g_R + (g_K + g_R)\frac{K^2}{I(I+1)}. \quad (5)$$

Prior to evaluating λ and μ, the values of g_K and Q_0 were determined as functions of the quadrupole deformation, ε_2. The intrinsic quadrupole moment as a function of deformation for ^{33}Mg was approximated classically as an ellipsoid from Ref. [36], where the ratio of the major and minor axes of the ellipsoid can be written as $((1+\frac{1}{3})\varepsilon_2)/(1-\frac{2}{3})$, and $q = \frac{2}{5}ZR^2$, with $R = r_0A^{1/3}$ and $r_0 = 1.2$ fm. The calculated values for Q_0 are shown in Table II.

In the Nilsson framework, the g-factor for an odd-A system can be separated into two components: g_K, which accounts for the motion of the odd neutron (in this case), and g_R, which describes the motion of the core. For ^{33}Mg, the odd-neutron g_K factor was calculated as

$$g_K = g_\ell + (g_s - g_\ell)\frac{< s_3 >}{K}, \quad (6)$$

where g_ℓ is the orbital angular momentum g-factor and is zero for neutrons, g_s is the spin g-factor and is -3.8263 for neutrons, and $< s_3 >$ is the projection of the spin onto the symmetry axis of the nucleus calculated as a function of deformation in a standard Nilsson code [34, 35]. The contribution of the core, described by g_R, is usually approximated by Z/A; measured values of g_R are typically comparable to, or slightly smaller than this approximation [26]. The Z/A approximation for ^{33}Mg yields a value of 0.36 for g_R; we ultimately consider g_R as an additional parameter that can be varied to optimize agreement with the data.

From the values of g_K and Q_0, both μ and λ were calculated as functions of deformation. After adjustment of g_R to a value of 0.30, λ, Q_0, and μ all show good agreement within a narrow range of ε_2 when compared to the experimental values. Table II summarizes the calculated parameters as well as the experimental values.

Table II: Parameters used to calculate the intensity ratio λ, ground-state magnetic moment (μ), and Q_0 of ^{33}Mg as a function of deformation (ε_2). The experimental values for λ, Q_0 [22], and μ [11] are shown in the last row of the table.

ε_2	g_K	Q_0 (eb)	$\mu(\mu_N)$	λ
0.2	-0.79	0.32	-0.53	0.048
0.3	-0.89	0.51	-0.62	0.10
0.4	0.99	0.74	-0.72	0.18
0.5	-1.04	1.01	-0.76	0.31
Experimental		0.7(0.16)	-0.7456(5)	0.24(8)

Figure 4 shows the calculations for λ, Q_0, and μ along with their experimental values (with shaded error bands). Due to the larger uncertainty on the experimental values of the intensity ratio (λ_{exp}) and intrinsic quadrupole moment (Q_0), there is a wide range of deformation where the calculated parameters for λ and Q_0 agree with their experimental values. This is denoted by the vertical, red and green bands in Figure 4, respectively. The uncertainty on the measured value of μ is small and therefore yields a narrower range of the deformation where the experimental and calculated values agree.

The agreement between these experimental observables and the simple leading order calculations presented here, for a reasonable deformation of 0.4 - 0.47, would seem to suggest that the tentative spins and parities presented in Table I are consistent, and the low-lying structure populated in ^{33}Mg can be described as a strongly-coupled rotational band.

We note that the results above were obtained using the free values for both $g_{\ell,free} = 0$ and $g_{s,free} = -3.8263$. Taking into account in-medium effects on the g-factors, we can also reproduce the data by considering the effective values $g_{\ell,eff} = -0.1$ and $g_{s,eff} = 0.9\ g_{s,free}$ which compensate the orbital and spin contributions to the magnetic moments, and is in line with the analysis in Refs. [26, 37, 38].

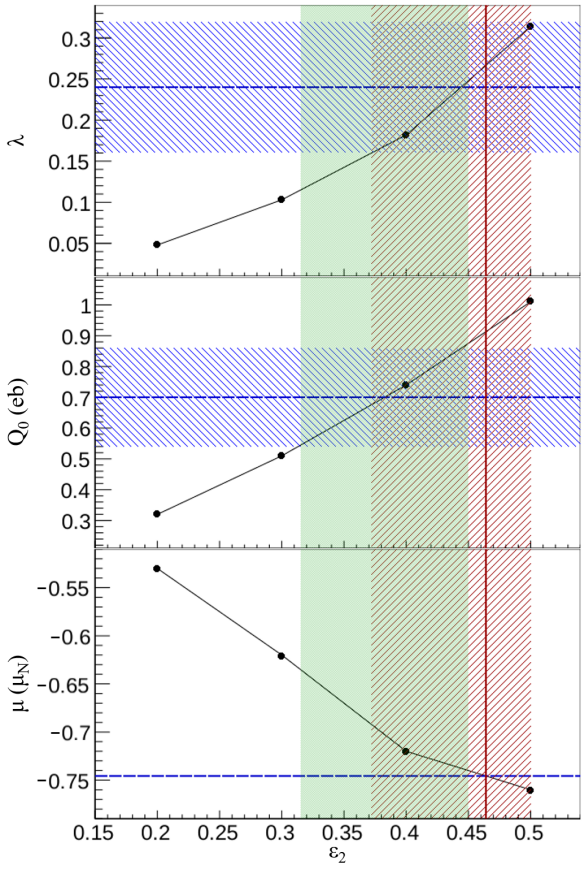

Figure 4: The calculations for λ, Q_0, and μ are shown in the three panels. The measured values are denoted with dashed blue lines with shaded error bands. The error band on the experimental value of μ is sufficiently small and appears as a line instead of an error band. The vertical red error band denotes the agreement range for the calculated λ and experimental value and the green vertical band denotes the range where the calculated Q_0 and the experimental value agree.

V. CONCLUSION

In summary, the low energy yrast states in ^{33}Mg were populated following a two-stage projectile fragmentation reaction and their de-excitation observed using GRETINA. Based upon $\gamma - \gamma$ coincidences and γ intensities, the level scheme was constructed, including placement of two new γ-ray transitions depopulating a new level at 780(6) keV. The experimental excitation energies, assuming tentative spin assignments built from $K = 3/2$ bandhead were compared to leading order approximations in the rotational framework in the strong coupling limit. A consistent picture emerges for excitation energies, the intensity ratio of the $E2/M1$ transitions depopulating the $(7/2^-)$ state, the intrinsic quadrupole moment, and the ground state magnetic moment as described within this simple framework. Within this description, we would predict the $9/2^-$ band member at

$\sim$1400 keV – further experimental effort is required to observe the $9/2^-$ and additional members in the ground-state rotational band, to further validate this description of ^{33}Mg.

Acknowledgments

This work was supported in part by the U.S. DOE through Grant No. DE-FG02-88ER40387 (OhioU), Contract No. DE-AC02-05CH11231 (LBNL), and Contract No. DE-AC02-06CH11357 (ANL). This material is based upon work supported by the U.S. Department of Energy, Office of Science, Office of Workforce Development for Teachers and Scientists, Office of Science Graduate Student Research (SCGSR) program. The SCGSR program is administered by the Oak Ridge Institute for Science and Education (ORISE) for the DOE. ORISE is managed by ORAU under contract number DEAC0506OR23100. GRETINA was funded by the U.S. DOE Office of Science. Operation of the array at NSCL is supported by NSF under Cooperative Agreement PHY11-02511 (NSCL) and DOE under Grant No. DE-AC02-05CH11231 (LBNL). We would like to thank the operations team and staff of the NSCL for all of their work in beam delivery and their assistance throughout the experiment.

[1] E.K. Warburton, J.A. Becker, B.A. Brown, Phys. Rev. C **41**, 1147 (1990).
[2] X. Campi, H. Flocard, A.K. Kerman, and S. Koonin, Nucl. Phys. A **251**, 193 (1975).
[3] C. Thibault, R. Klapisch, C. Rigaud, A.M. Poskanzer, R. Prieels, L. Lessard, and W. Reisdorf, Phys. Rev. C **12**, 644 (1975).
[4] G. Huber, F. Touchard, S. Büttgenbach, C. Thibault, R. Klapisch, H. T. Duong, S. Liberman, J. Pinard, J. L. Vialle, P. Juncar, et al., Phys. Rev. C **18**, 2342 (1978).
[5] C. Detraz, M. Langevin, M.C. Goffri-Kouassi, D. Guillemaud, M. Epherre, G. Audi, C. Thibault, and F. Touchard, Nucl. Phys. A **394**, 378 (1983).
[6] B.H. Wildenthal, M.S. Curtin, and B.A. Brown, Phys. Rev. C **28**, 1343 (1983).
[7] D. Guillemaud-Mueller, C. Detraz, M. Langevin, F. Naulin, M. de Saint-Simon, C. Thibault, F. Touchard, and M. Epherre, Nucl. Phys. A **426**, 37 (1984).
[8] A. Poves, J. Retamosa, Phys. Lett. B **184**, 311 (1987).
[9] O. Sorlin, M.G. Porquet, Prog. Part. and Nucl. Phys. **61**, 602 (2008).
[10] H. L. Crawford, P. Fallon, A. O. Macchiavelli, A. Poves, V. M. Bader, D. Bazin, M. Bowry, C. M. Campbell, M. P. Carpenter, R. M. Clark, et al., Phys. Rev. C **93**, 031303 (2016).
[11] D. T. Yordanov, M. Kowalska, K. Blaum, M. De Rydt, K. T. Flanagan, P. Lievens, R. Neugart, G. Neyens, and H. H. Stroke, Phys. Rev. Lett. **99**, 212501 (2007).
[12] M. Kowalska, D. T. Yordanov, K. Blaum, P. Himpe, P. Lievens, S. Mallion, R. Neugart, G. Neyens, and N. Vermeulen, Phys. Rev. C **77**, 034307 (2008).
[13] U. Datta, A. Rahaman, T. Aumann, S. Beceiro-Novo, K. Boretzky, C. Caesar, B. V. Carlson, W. N. Catford, S. Chakraborty, M. Chartier, et al., Phys. Rev. C **94**, 034304 (2016).
[14] S. Paschalis, I. Y. Lee, A. O. Macchiavelli, C. M. Campbell, M. Cromaz, S. Gros, J. Pavan, J. Qian, R. M. Clark, H. L. Crawford, et al., Nucl. Instrum. Methods Phys. Res., Sect. A **709**, 44 (2013).
[15] D. Morrissey, B.M. Sherrill, M. Steiner, A. Stolz, and I. Wiedenhoever, Nucl. Instrum. Methods Phys. Res., Sect. B **204**, 90 (2003).
[16] D. Bazin, J.A. Caggiano, B.M. Sherrill, J. Yurkon, and A. Zeller, Nucl. Instrum. Methods Phys. Res., Sect. B **204**, 629 (2003).
[17] J. Yurkon, D. Bazin, W. Benenson, D.J. Morrissey, B.M. Sherrill, D. Swan, and R. Swanson, Nucl. Instrum. Methods Phys. Res., Sect. A **422**, 291 (1999).
[18] K. Meierbachtol, D. Bazin, and D.J. Morrissey, Nucl. Instrum. Methods Phys. Res., Sect. A **652**, 668 (2011).
[19] L. Riley *et al.*, to be published.
[20] K. Yoneda, H. Sakurai, T. Gomi, T. Motobayashi, N. Aoi, N. Fukuda, U. Futakami, Z. Gacsi, Y. Higurashi, N. Imai, et al., Phys. Lett. B **499**, 233 (2001).
[21] S. Nummela, F. Nowacki, P. Baumann, E. Caurier, J. Cederkäll, S. Courtin, P. Dessagne, A. Jokinen, A. Knipper, G. Le Scornet, et al., Phys. Rev. C **64**, 054313 (2001).
[22] B. V. Pritychenko, T. Glasmacher, P. D. Cottle, R. W. Ibbotson, K. W. Kemper, L. A. Riley, A. Sakharuk, H. Scheit, M. Steiner, and V. Zelevinsky, Phys. Rev. C **65**, 061304 (2002).
[23] Z. Elekes, Z. Dombrádi, A. Saito, N. Aoi, H. Baba, K. Demichi, Z. Fülöp, J. Gibelin, T. Gomi, H. Hasegawa, et al., Phys. Rev. C **73**, 044314 (2006).
[24] T. Fukui, S. Ota, S. Shimoura, N. Aoi, E. Takeshita, S. Takeuchi, H. Suzuki, H. Baba, T. Fukuchi, Y. Hashimoto, et al., Tech. Rep. CNS-REP-69,P19 (2006).
[25] D. T. Yordanov for the COLLAPS Collaboration, Hyperfine Interactions **196**, 53 (2010).
[26] A. Bohr and B. Mottelson, *Nuclear Structure*, vol. II (W. A. Benjamin, Inc., Advanded Book Program, Reading, 1975).
[27] C. Détraz, D. Guillemaud, G. Huber, R. Klapisch, M. Langevin, F. Naulin, C. Thibault, L. C. Carraz, and F. Touchard, Phys. Rev. C **19**, 164 (1979).
[28] T. Motobayashi, Y. Ikeda, K. Ieki, M. Inoue, N. Iwasa, T. Kikuchi, M. Kurokawa, S. Moriya, S. Ogawa, H. Murakami, et al., Phys. Lett. B **346**, 9 (1995).
[29] B. V. Pritychenko, T. Glasmacher, P. D. Cottle, M. Fauerbach, R. W. Ibbotson, K. W. Kemper, V. Maddalena, A. Navin, R. Ronningen, A. Sakharuk, et al., Phys. Lett. B **461**, 322 (1999).
[30] V. Chiste, A. Gillibert, A. Lpine-Szily, N. Alamanos, F. Auger, J. Barrette, F. Braga, M. Cortina-Gil, Z. Dlouhy, V. Lapoux, et al., Phys. Lett. B **514**, 233 (2001).

[31] J. A. Church, C. M. Campbell, D. C. Dinca, J. Enders, A. Gade, T. Glasmacher, Z. Hu, R. V. F. Janssens, W. F. Mueller, H. Olliver, et al., Phys. Rev. C **72**, 054320 (2005).
[32] S. Takeuchi, N. Aoi, T. Motobayashi, S. Ota, E. Takeshita, H. Suzuki, H. Baba, T. Fukui, Y. Hashimoto, K. Ieki, et al., Phys. Rev. C **79**, 054319 (2009).
[33] H. Iwasaki, T. Motobayashi, H. Sakurai, K. Yoneda, T. Gomi, N. Aoi, N. Fukuda, Z. Flp, U. Futakami, Z. Gacsi, et al., Phys. Lett. B **522**, 227 (2001).
[34] S. G. Nilsson, Selsk. Mat. Fys. Medd. **16**, 29 (1955).
[35] S. Larsson, G. Leander, and I. Ragnarsson, Nucl. Phys. A **307**, 189 (1978).
[36] L.D. Landau, E.M. Lifshitz, and L.P. Pitaevskii, *Electrodynamics of Continuous Media* (Pergamon, New York, 1984), 2nd ed.
[37] B. A. Brown and B. Wildenthal, Ann. Rev. Nucl. Part. Sci. **38**, 29 (1988).
[38] W. Bentz and A. Arima, Science China **53**, 1 (2010).